Weak Gravitational Lensing from Theory to Observations

Marika Asgari, July 2025, Observational Cosmology school at Institute of Space Sciences

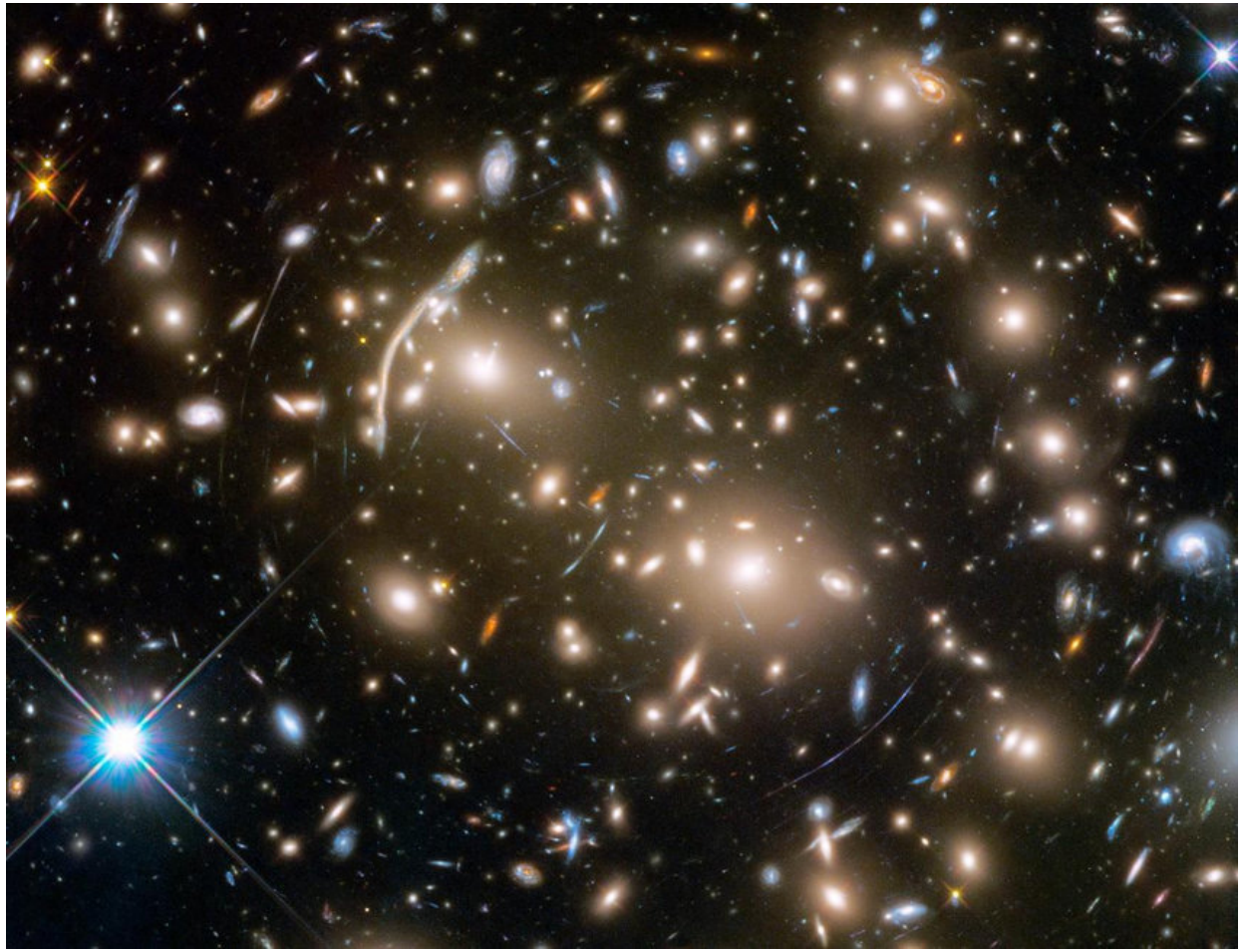

Figure 1. Abel 370 cluster, as imaged by the Hubble Space Telescope.

The standard theory of gravity is general relativity, which expresses how matter and energy shape the space-time. The light of a far away galaxy travels through space-time which is affected by the presence of large scale structures and the general geometry of the Universe. According to general relativity light travels through the shortest path between two points in space-time or along geodesics. Therefore, the distortions caused by matter and energy to space-time, change the path of light. We can see this effect in the distorted images of galaxies. This is the fundamental idea behind gravitational lensing.

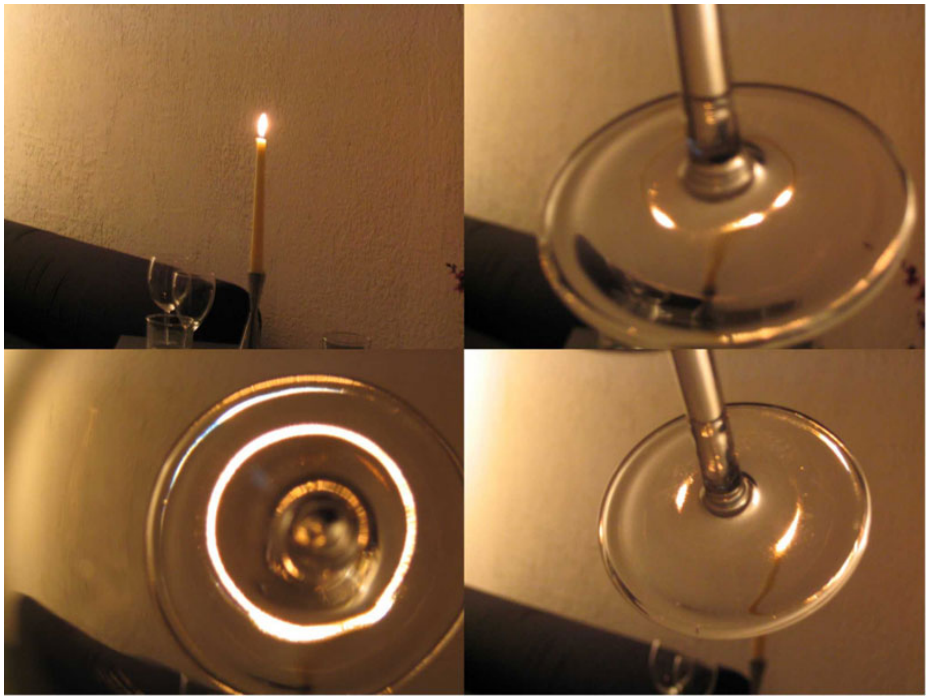

Figure 2. A wine glass and a light source is all you need to simulate gravitational lensing effects. The bottom left photo shows the "Einstein Ring", where the light of the candle is aligned with the center of the glass. The right panels show multiple images of the candle. These phenomena resemble strong lensing effects of massive gravitational lenses on background light sources such as galaxies further away from us.

In most astrophysical situations a gravitational lens acts very much like an optical lens, and is sometimes called a cosmic telescope. The distortion of galaxy images can be strong, in which case more than one image of the same galaxy will be visible, or weak, where the images are only slightly sheared. These effects can be simulated using a wine glass and a small light source like a candle as in Fig. 2. In these lectures we will derive some of the basics of this gravitational lens theory, which we will then build upon in the weak lensing regime.

1. Lens Equation

The lens equation is the fundamental equation that governs the gravitational lensing effects. Considering a typical lensing system as in Fig. 3:

You can use Figure 3 to show

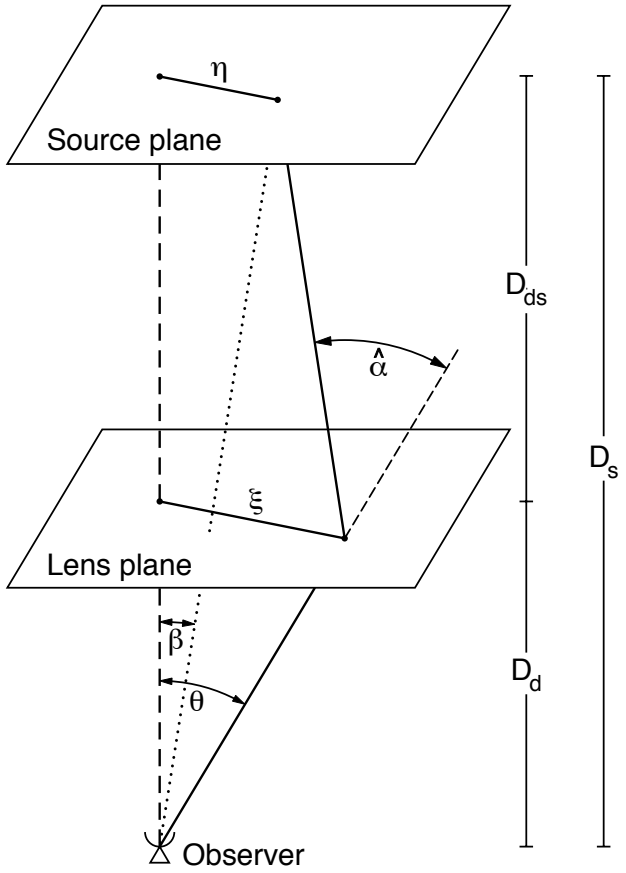

Figure 3. Sketch of a gravitational lensing system, taken from Bartelmann & Schneider 2001. The distances between the observer, the lens and the source planes are calculated in terms of angular diameter distance. The lens changes the position angle of the source from β to θ, as seen by the observer

$$\boldsymbol{\theta}\mathrm{D_s} = \boldsymbol{\beta}\mathrm{D_s} + \hat{\boldsymbol{\alpha}}\mathrm{D_{ds}}. \tag{1}$$

and the lens equation:

$$\boldsymbol{\beta} = \boldsymbol{\theta} - \frac{D_{\mathrm{ds}}}{D_{\mathrm{s}}}\hat{\boldsymbol{\alpha}}(D_{\mathrm{d}}\boldsymbol{\theta}) \equiv \boldsymbol{\theta} - \boldsymbol{\alpha}(\boldsymbol{\theta}) \ , \tag{2}$$

where β is the source position on the sky (not an observable), $\boldsymbol{\theta}$ is the image position (observable), and $\boldsymbol{\alpha}$ is the scaled deflection angle. The lens equation is valid for the weak field regime, and thin lenses, which corresponds to mass distributions which have a small line-of-sight span compared to the distances between the observer, the lens and the source.

The most basic equation relevant for gravitational lensing is the relation between the deflection angle, $\hat{\alpha}$, of a light ray passing a spherically symmetric body of mass M with an impact parameter, ξ, where ξ is much larger than the Schwarzschild radius, $R_{\rm s} \equiv 2GM/c^2$,

$$\hat{\alpha} = \frac{4GM}{c^2\xi} \ . \tag{3}$$

The deflection angle obtained here is a factor of two larger than that expected from Newtonian physics.

Assumption 1: For a mass distribution the aforementioned equation can be generalized, since in the **weak-field limit** the sum of the deflection angles from mass elements is equal to the total deflection angle from the total mass.

Assumption 2: For a **thin lens** we can assume that the light ray is a straight line in the vicinity of the lens and the deflection happens on the lens plane. Although we have made a second assumption that the lens is thin, it can still be extended. In this case $\hat{\alpha}$ can be written in terms of the sum of the deflection angles from small lens mass elements at position $\boldsymbol{r}' = (\xi_1', \xi_2', r_3')$ (prime is used to show the lens element positions),

$$\mathrm{d}m = \mathrm{d}^2\xi' \mathrm{d}r_3' \ \rho(\boldsymbol{r}') \ , \tag{4}$$

where $\boldsymbol{\xi} = D_{\rm d}\boldsymbol{\theta}$ is the position vector on the lens plane, while r_3 shows the position in the line-of-sight direction, perpendicular to the lens plane.

If the light ray has an impact vector of $\boldsymbol{\xi} = (\xi_1, \xi_2)$ then Eq. (3) reads,

$$\hat{\boldsymbol{\alpha}} = \frac{4G}{c^2} \int \mathrm{d}m \frac{\boldsymbol{\xi} - \boldsymbol{\xi}'}{|\boldsymbol{\xi} - \boldsymbol{\xi}'|^2} \ , \tag{5}$$

$$\hat{\boldsymbol{\alpha}} = \frac{4G}{c^2} \int \mathrm{d}^2\xi' \int \mathrm{d}r_3' \ \rho(\boldsymbol{r}') \frac{\boldsymbol{\xi} - \boldsymbol{\xi}'}{|\boldsymbol{\xi} - \boldsymbol{\xi}'|^2} \ , \tag{6}$$

where $\hat{\boldsymbol{\alpha}}$ is a two dimensional vector. Since $\rho(\boldsymbol{r}')$ is the only quantity in the above equation that depends on r_3', the line-of-sight integral can be taken independent of the source position. As a result, we can define a surface mass density for the lens as follows,

$$\Sigma(\boldsymbol{\xi}) \equiv \int \mathrm{d}r_3' \; \rho(\xi_1', \xi_2', r_3') \; . \tag{7}$$

Let us define the dimensionless surface mass density (convergence) as,

$$\kappa(\boldsymbol{\theta}) \equiv \frac{\Sigma(D_\mathrm{d}\boldsymbol{\theta})}{\Sigma_\mathrm{cr}} \text{ with } \Sigma_\mathrm{cr} = \frac{c^2}{4\pi G} \frac{D_\mathrm{s}}{D_\mathrm{d} D_\mathrm{ds}} \; , \tag{8}$$

where Σ_cr is the critical surface mass density which depends on the distances between the observer, the lens and the source (see Fig. 3).

Q: Write $\boldsymbol{\alpha}(\boldsymbol{\theta})$ in terms of the convergence.

$$\hat{\boldsymbol{\alpha}} = \frac{4G}{c^2} \int \mathrm{d}^2\xi' \int \mathrm{d}r_3' \; \rho(\boldsymbol{r}') \frac{\boldsymbol{\xi} - \boldsymbol{\xi}'}{|\boldsymbol{\xi} - \boldsymbol{\xi}'|^2} \; , \tag{9}$$

$$\boldsymbol{\beta} = \boldsymbol{\theta} - \frac{D_\mathrm{ds}}{D_\mathrm{s}} \hat{\boldsymbol{\alpha}}(D_\mathrm{d}\boldsymbol{\theta}) \equiv \boldsymbol{\theta} - \boldsymbol{\alpha}(\boldsymbol{\theta}) \; , \tag{10}$$

We can rewrite Eq. (5) for the scaled deflection angle,

$$\boldsymbol{\alpha}(\boldsymbol{\theta}) = \frac{1}{\pi}\int_{R^2} \mathrm{d}\theta'^2\, \kappa(\boldsymbol{\theta'})\frac{\boldsymbol{\theta}-\boldsymbol{\theta'}}{|\boldsymbol{\theta}-\boldsymbol{\theta'}|^2}\ , \tag{11}$$

Using the identity

$$\nabla_\theta \ln(\boldsymbol{\theta}-\boldsymbol{\theta'}) = \frac{\boldsymbol{\theta}-\boldsymbol{\theta'}}{|\boldsymbol{\theta}-\boldsymbol{\theta'}|^2} \tag{12}$$

we can rewrite Eq. (23) as the gradient of a deflection potential, $\psi(\boldsymbol{\theta})$,

$$\boldsymbol{\alpha}(\boldsymbol{\theta}) = \frac{1}{\pi}\int_{R^2} \mathrm{d}\theta'^2\, \kappa(\boldsymbol{\theta'})\nabla_\theta \ln(\boldsymbol{\theta}-\boldsymbol{\theta'}) = \nabla_\theta\psi(\boldsymbol{\theta})\ .$$

In addition, via

$$\nabla^2 \ln|\boldsymbol{\theta}| = 2\pi\delta_D(\boldsymbol{\theta}), \tag{13}$$

a Poisson equation for the deflection potential and the convergence is obtained,

$$\nabla^2\psi = \nabla.\boldsymbol{\alpha} = 2\kappa\ . \tag{14}$$

2. Mapping between the source and lens planes

Liouville's theorem, in basic terms, says that our lensed photon bundles evolve in the same way in time, and will therefore have a density that does not change with time. This combined with the absence of any photon emission or absorption process in gravitational lensing implies that lensing conserves surface brightness. Therefore if gravitational lensing increases the area of an image we will see magnification μ where

$$\mu = \frac{\text{image area}}{\text{source area}} = \frac{\mathrm{d}^2\theta}{\mathrm{d}^2\beta}, \tag{15}$$

for an element of source $\delta\beta^2$ mapped onto an area of image $\delta\theta^2$. Note that lensing effectively focuses the light from a source. For a lensed source we receive photons that we would have detected in the absence of the lens, plus additional photons on previously nearby trajectories that are now bent into the detector by the lens.

Considering an infinitesimally small source (one that is much smaller than the angular scale on which the lens properties change), the lens mapping can be described by the lensing 'Jacobian'

$$\mathcal{A}(\boldsymbol{\theta}) = \frac{\partial \boldsymbol{\beta}}{\partial \boldsymbol{\theta}} = \delta_{ij} - \frac{\partial^2 \psi(\boldsymbol{\theta})}{\partial\theta_i\,\partial\theta_j} = \delta_{ij} - \psi_{,ij} \tag{16}$$

$$\mathcal{A}(\boldsymbol{\theta}) = \begin{pmatrix} 1-\kappa-\gamma_1 & -\gamma_2 \\ -\gamma_2 & 1-\kappa+\gamma_1 \end{pmatrix}, \tag{17}$$

What is the relation between $\gamma_{1,2}$ and ψ?

What is the relation between μ and $\mathcal{A}$?

Here is how ψ is related to shear and convergence:

$$\begin{aligned} \kappa &\equiv \quad (\psi_{,11} + \psi_{,22})/2 \\ \gamma_1 &\equiv \quad (\psi_{,11} - \psi_{,22})/2 \\ \gamma_2 &\equiv \quad \psi_{,12}, \end{aligned} \tag{18}$$

We can define

$$\gamma \equiv \gamma_1 + \mathrm{i}\gamma_2 = e^{2i\varphi}, \tag{19}$$

as a two component quantity. Note that γ is not a vector, but a polar. Because it only needs to turn 180 degrees to turn back on itself. We will take a closer look at this in the next section.

The magnification is given by the determinant of the inverse of A (start from Eq. 15 and the Jacobian) ,

$$\mu = \frac{1}{\det \mathcal{A}} = \frac{1}{(1-\kappa)^2 - \gamma^2}\,. \tag{20}$$

Note that μ as defined above has a sign which relates to the type of image observed.

We will now define the reduced shear

$$g = \gamma/(1-\kappa) \tag{21}$$

such that

$$A = (1-\kappa)\begin{pmatrix} 1-g_1 & -g_2 \\ -g_2 & 1+g_1 \end{pmatrix}, \tag{22}$$

showing the convergence κ only affects the size of the image and hence its magnification, whereas shear is responsible for image distortions changing the shape or ellipticity of the image.

When we solve the lens equation, we sometimes get multiple solutions or singularities, where the determinant of the Jacobean is zero. The singular solutions produce curves in the lens plane called critical curves and corresponding curves in the source plane called caustics. The critical curves are generally smooth, but caustics can have sharp points. When a source crosses a caustic it produces another two images in the lens plane. Fig. 4 shows how different source positions affect the images.

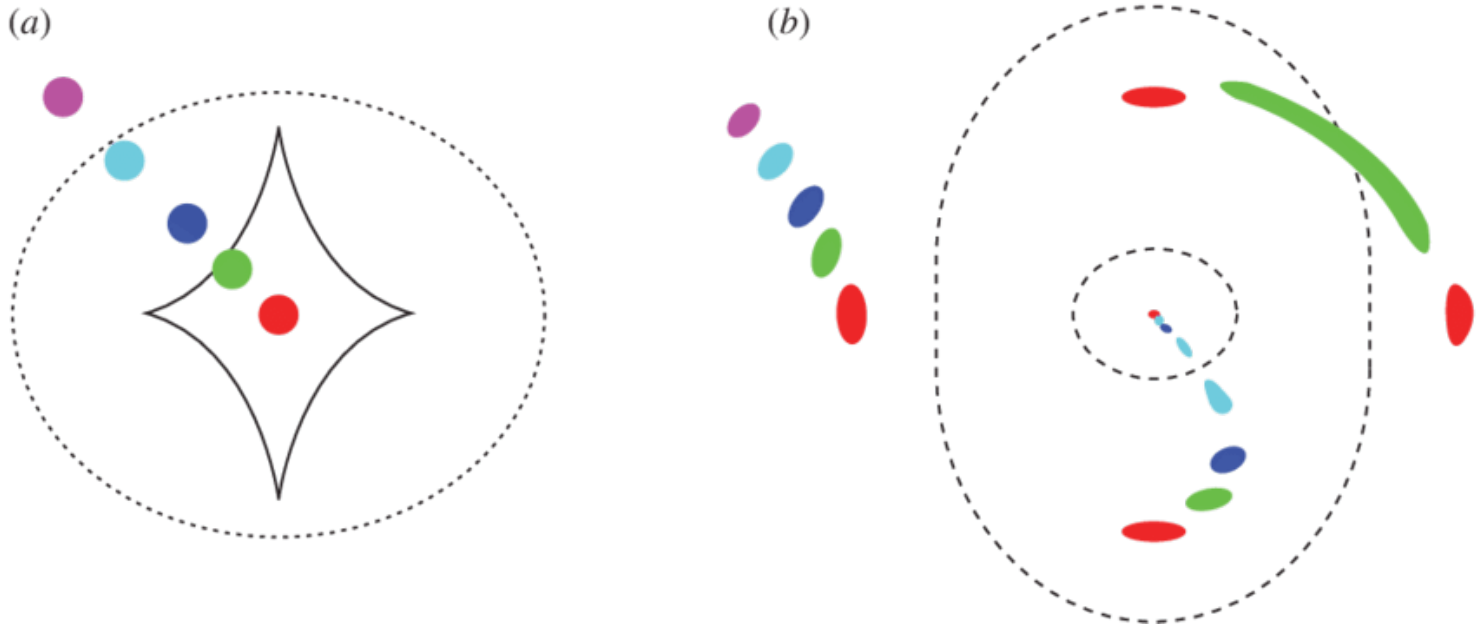

Figure 4. A sketch of critical curves and caustics. Panel a shows the source place while panel b shows the image plane. Adopted from Ellis et al. (2010). Note that the inner most blue point, near the red point in the middle, should be green.

3. The case of the axially symmetric lens

In the special case of an axially symmetric lens characterized by $\kappa(\boldsymbol{\theta}) = \kappa(|\boldsymbol{\theta}|)$, we can choose the origin of our co-ordinate system as the centre of symmetry, and the reduced deflection angle now just depends on the distance from the centre of the lens;

$$\boldsymbol{\alpha}(\boldsymbol{\theta}) = \frac{1}{\pi} \int_{R^2} \mathrm{d}\theta'^2 \, \kappa(\boldsymbol{\theta'}) \frac{\boldsymbol{\theta - \theta'}}{|\boldsymbol{\theta - \theta'}|^2} \ , \tag{23}$$

$$\boldsymbol{\alpha}(\boldsymbol{\theta}) = \frac{\boldsymbol{\theta}}{|\boldsymbol{\theta}|^2} \frac{2\pi}{\pi} \int \mathrm{d}\theta' \, \theta' \, \kappa(\theta') \, , \tag{24}$$

where $\theta = |\boldsymbol{\theta}|$. Defining the mean convergence $\bar{\kappa}$ as

$$\bar{\kappa}(\theta) = \frac{2}{|\boldsymbol{\theta}|^2} \int_0^\theta \mathrm{d}\theta' \, \theta' \, \kappa(\theta') \, , \tag{25}$$

we find

$$\boldsymbol{\alpha}(\boldsymbol{\theta}) = \boldsymbol{\theta} \, \bar{\kappa}(\theta) \, , \tag{26}$$

and hence the lens equation for an axially symmetric lens is

$$\boldsymbol{\beta} = \boldsymbol{\theta} \left[1 - \bar{\kappa}(\theta) \right] \ . \tag{27}$$

4. Shear from an axially symmetric lens

In equation 27 we derived the lens equation for an axially symmetric lens.

What is the Jacobian in this case?

(28) $$\mathcal{A}(\boldsymbol{\theta}) = \frac{\partial \boldsymbol{\beta}}{\partial \boldsymbol{\theta}}$$

Lens equation for an axially symmetric lens:

$$\boldsymbol{\beta} = \boldsymbol{\theta}\left[1 - \bar{\kappa}(|\boldsymbol{\theta}|)\right] , \quad \bar{\kappa}(\theta) = \frac{2}{|\boldsymbol{\theta}|^2}\int_0^\theta d\theta'\,\theta'\,\kappa(\theta') ,$$

Find the reduced shear.

(29) $$A = (1-\kappa)\begin{pmatrix} 1-g_1 & -g_2 \\ -g_2 & 1+g_1 \end{pmatrix},$$

You can use these eqs:

(30) $$\bar{\kappa}'(\theta) = \frac{\mathrm{d}\bar{\kappa}(\theta)}{\mathrm{d}\theta} = \frac{2}{\theta}\left[\kappa(\theta) - \bar{\kappa}(\theta)\right].$$

$$\theta_1 = \theta\cos\phi, \quad \theta_2 = \theta\sin\phi, \quad \cos^2\phi = \frac{1}{2}(1+\cos 2\phi).$$

Solution:

Lets take the first term

$$A_{11} = \frac{\partial \beta_1}{\partial \theta_1} \,. \tag{31}$$

we know

$$\beta_1 = \theta_1 - \bar{\kappa}(|\boldsymbol{\theta}|)\theta_1 \tag{32}$$

and hence

$$A_{11} = 1 - \bar{\kappa}(|\boldsymbol{\theta}|) - \frac{\theta_1^2}{|\boldsymbol{\theta}|}\bar{\kappa}'(|\boldsymbol{\theta}|)\,, \tag{33}$$

where

$$\bar{\kappa}'(\theta) = \frac{\mathrm{d}\bar{\kappa}(\theta)}{\mathrm{d}\theta} = \frac{2}{\theta}\left[\kappa(\theta) - \bar{\kappa}(\theta)\right]. \tag{34}$$

You can calculate each component of the Jacobian in this way and you'll find

$$A = (1-\bar{\kappa})\begin{pmatrix} 1 & 0 \\ 0 & 1 \end{pmatrix} - \frac{\bar{\kappa}'}{\theta}\begin{pmatrix} \theta_1^2 & \theta_1\theta_2 \\ \theta_1\theta_2 & \theta_2^2 \end{pmatrix}. \tag{35}$$

Compare this derived Jacobian with equation 29 you can find expressions for the shear around an axially symmetric lens, in terms of the convergence (which remember is the projected surface mass density).

$$\begin{pmatrix} g_1(\phi) \\ g_2(\phi) \end{pmatrix} = \kappa - \bar{\kappa} \begin{pmatrix} \cos 2\phi \\ \sin 2\phi \end{pmatrix}, \tag{36}$$

where $\theta_1 = \theta \cos\phi$ and $\theta_2 = \theta \sin\phi$. To get to this you'll need to use $\cos^2\phi = \frac{1}{2}(1 + \cos 2\phi)$.

5. Example: The Simple Isothermal Sphere Model

A model that is often used to describe the density of dark matter haloes is the singular isothermal sphere (SIS);

$$\rho(r) = \frac{\sigma_v^2}{2\pi G r^2} \tag{37}$$

where σ_v is the velocity dispersion of the halo. This profile produces flat rotation curves but is singular in the centre ($r \to 0$, $\rho \to \infty$) and and the total mass diverges at large radii ($r \to \infty$). It is therefore usual to also include a truncation radius where $\rho(> r_T) = 0$ and a different relation for the inner most regions (see NFW profile for example).

What lensing effects do we expect to observe around a SIS?

Using the symmetry of the lens, setting our co-ordinate origin at the centre of the SIS halo, the projected surface mass density becomes,

$$\Sigma(\xi) = \int_{-\infty}^{\infty} \mathrm{d}r_3 \, \frac{\sigma_v^2}{2\pi G(\xi^2 + r_3^2)} = \frac{\sigma_v^2}{2G\,\xi} \tag{38}$$

The convergence is then

(39)
$$\kappa = \frac{\Sigma(\mathrm{D_d}\theta)}{\Sigma_{\mathrm{cr}}} = \frac{2\pi\,\sigma_v^2}{c^2}\,\frac{D_{\mathrm{ds}}}{D_{\mathrm{s}}\theta}$$

and the reduced shear tangential to the lens is given by equation 36,

(40)
$$g = \bar{\kappa} - \kappa = \frac{2\pi\,\sigma_v^2}{c^2}\,\frac{D_{\mathrm{ds}}}{D_{\mathrm{s}}\theta}$$

by calculating $\bar{\kappa}$ using equation 25 to find that in this case $\bar{\kappa} = 2\kappa$.

In practise we would use an 'NFW' halo model, rather than a SIS, see Wright & Brainerd 2000 if you're interested in the derivation for a more complex halo density profile. For a typical spiral galaxy halo the lensing shear is very weak $\gamma \sim 0.005$. Compare this to the intrinsic galaxy ellipticity which has a distribution $< e^2 > \sim 0.3$. This weakly induced distortion is therefore very difficult to measure and can only be measured statistically by stacking the lensing signal around many thousands of halos. This is known as 'galaxy-galaxy' lensing, illustrated in figure **??**.

Find the Einstein ring expression in terms of the image position for this lens.

The Einstein ring occurs at the singular solution for the lens equations. For such an axially symmetric lens that happens when the sources is right behind the lens.

$$\boldsymbol{\beta} = \boldsymbol{\theta}\left[1 - \bar{\kappa}(|\boldsymbol{\theta}|)\right]\,, \quad \bar{\kappa}(\theta) = \frac{2}{|\boldsymbol{\theta}|^2}\int_0^{\theta} d\theta'\,\theta'\,\kappa(\theta')\,,$$

Solution

(41)
$$\theta_{\mathrm{E}} = 4\pi(\sigma_v/c)^2 D_{\mathrm{ds}}/D_{\mathrm{s}}$$

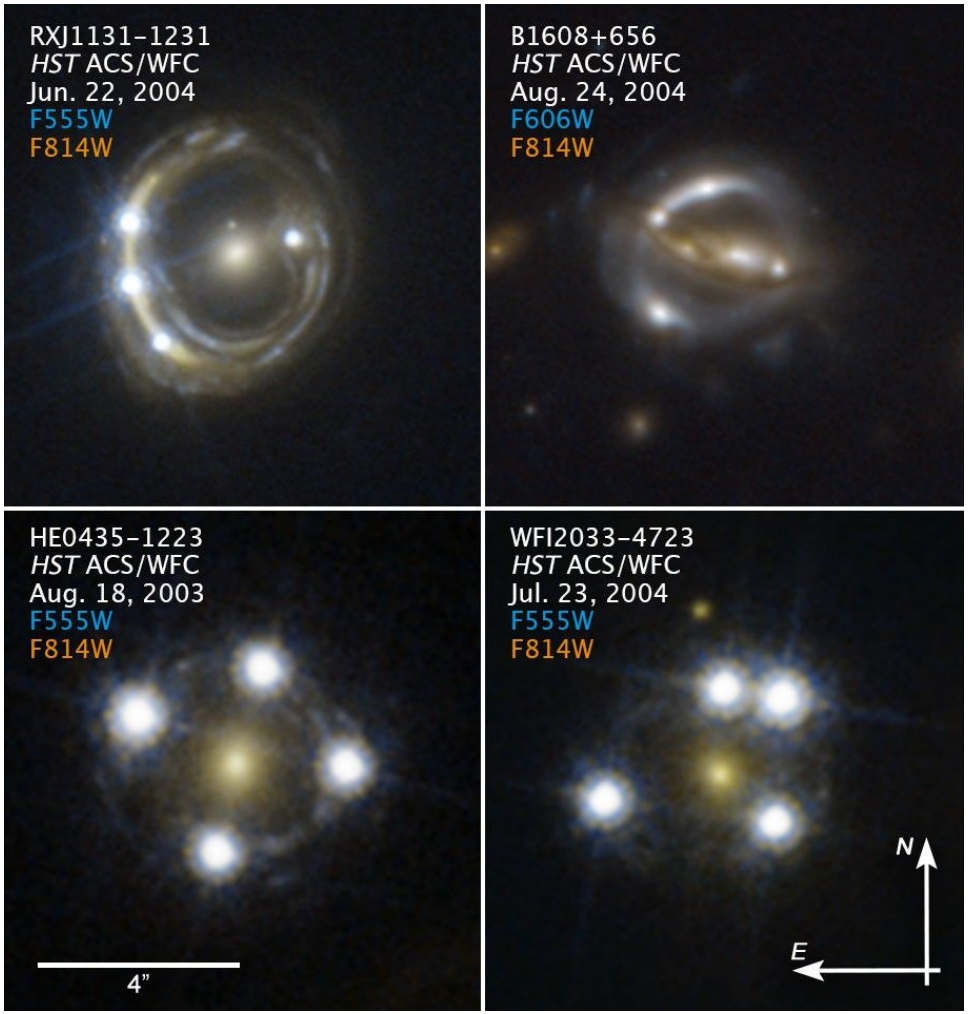

Figure 5. Einstein ring and multiple images of quasars.

6. Shear and Ellipticity

Visually the convergence and shear impact the image in different manners. As we saw with the Jacobean κ applies an isotropic magnification to the image, while shear (or rather reduced shear) stretches the image. Fig. 6 shows what happens to a circular source.

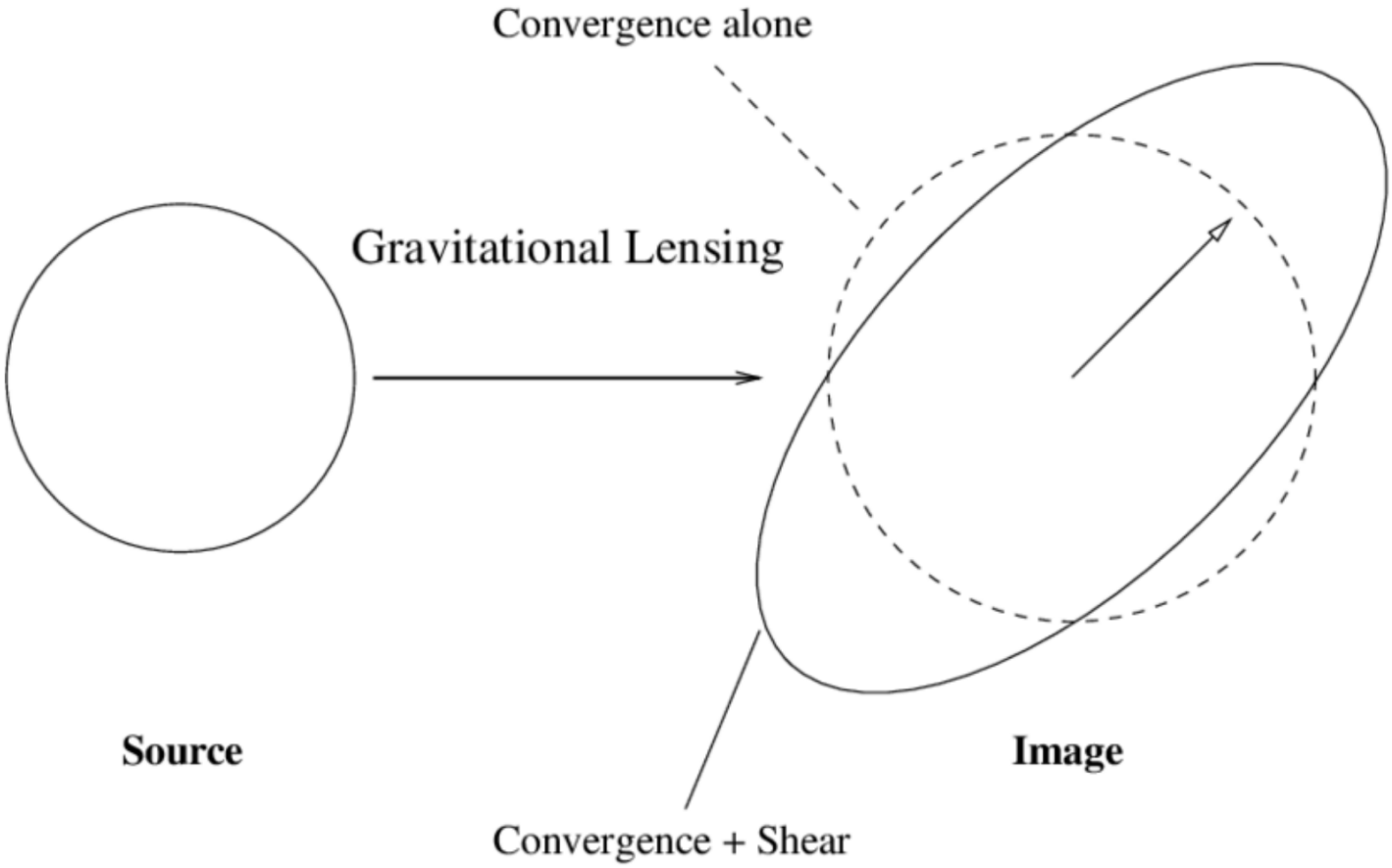

Figure 6. A sketch of how a circular source is impacted by shear and convergence.

However we know that galaxies are generally not circular and have their own intrinsic shape which also depends on their relative orientation to the observer. In weak lensing observations the galaxies are approximated by ellipses, and characterized by their ellipticity a two component quantity that is defined similar to shear. Fig. 7 shows how ellipticity complicates the analysis of weak lensing data. The intrinsic ellipticity of the galaxies is a source of noise in weak lensing data.

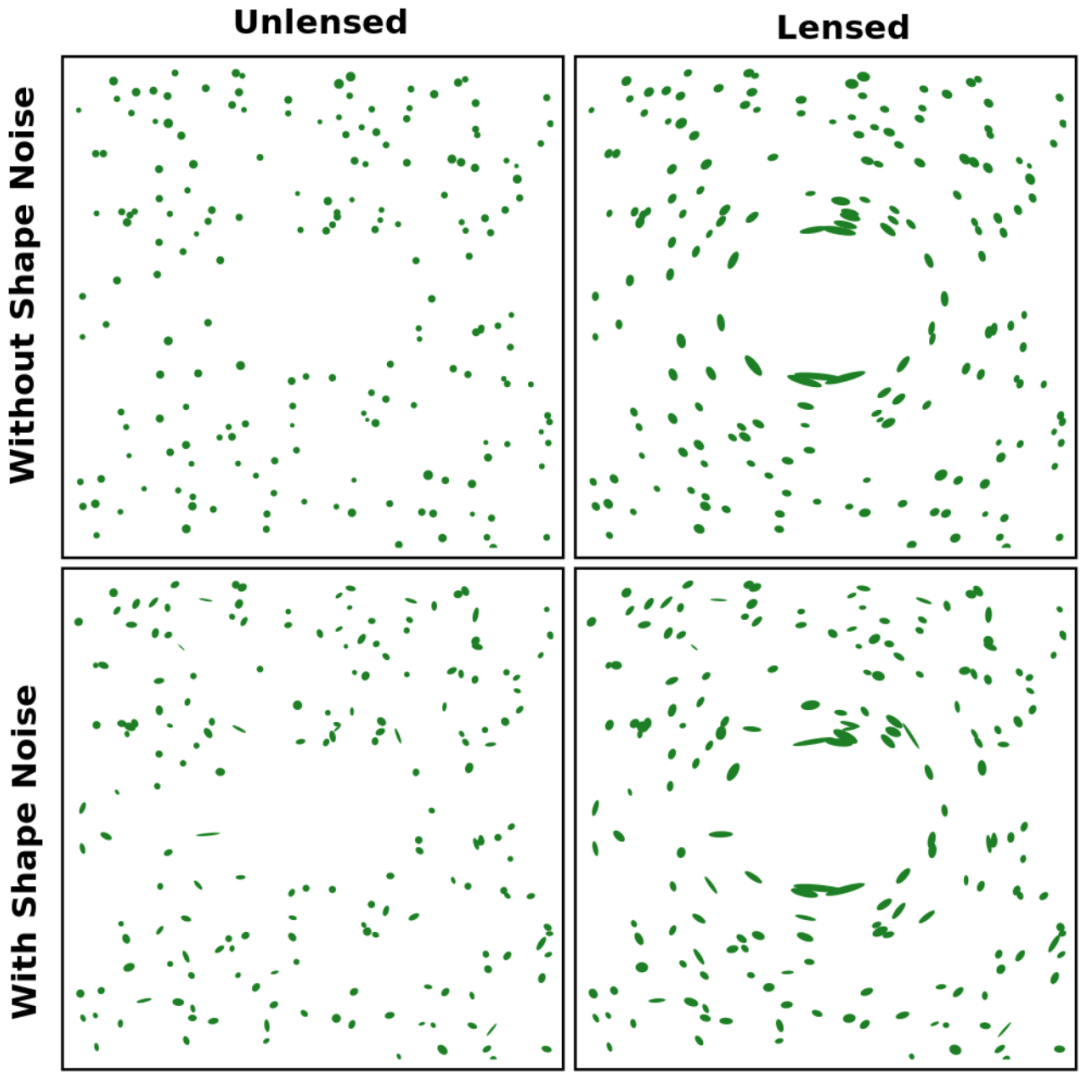

Figure 7. Background galaxy distribution with and without a foreground lens or with and without shape noise

Like shear, ellipticity, ϵ, can be written as a complex quantity,

$$\epsilon = \epsilon_1 + i\epsilon_2 \ . \tag{42}$$

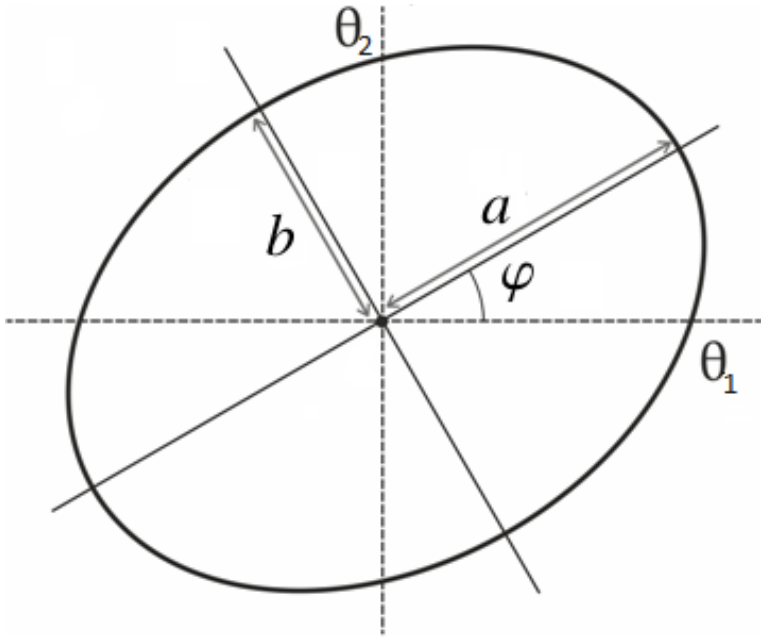

Figure 8. A galaxy image is estimated by an ellipse for weak gravitational lensing. The ellipse is characterized by its semi-major and minor axes, a and b, and its orientation, φ with respect to the reference frame.

For the configuration in Fig. 8 the two components of the ellipticity are defined as,

$$\begin{pmatrix} \epsilon_1 \\ \epsilon_2 \end{pmatrix} = \frac{1-r}{1+r} \begin{pmatrix} \cos(2\varphi) \\ \sin(2\varphi) \end{pmatrix}, \tag{43}$$

where

$$r = a/b. \tag{44}$$

The observed ellipticity of a galaxy depends on the reduced shear,

$$g = \frac{\gamma}{1-\kappa} \ . \tag{45}$$

The expectation value of the observed ellipticity in the absence of any systematical errors in the weak lensing regime is,

$$\left\langle \epsilon^{\rm obs} \right\rangle = \left\langle \epsilon^{\rm int} \right\rangle + \left\langle g \right\rangle \ , \tag{46}$$

where $\langle \epsilon^{\rm int} \rangle$ will give rise to a shot noise term for the covariance.

The shear defined above is in Cartesian coordinates, however, for practical reasons shear is usually defined with respect to a rotated reference frame. If ϕ is the orientation of the rotated frame, the tangential and the cross components of the shear are defined as follows,

$$\gamma_{\rm t} = -{\rm Re}(\gamma\, {\rm e}^{-2{\rm i}\phi}) \ , \qquad \gamma_\times = -{\rm Im}(\gamma\, {\rm e}^{-2{\rm i}\phi}) \ . \tag{47}$$

In the following sections we will expand the general formalism of gravitational lensing explained here to cosmological scales. Gravitational lensing has many other applications from microlensing which is used for finding exoplanets, galaxy-galaxy lensing which provides information about the environment in which galaxies reside, to lensing by clusters of galaxies which yield a robust measure of cluster mass distribution.

7. Very Weak Gravitational Lensing

In the very weak distortion regime relevant for comic shear, both the convergence and shear are small, and the expectation value of the ellipticity of the images is approximated by shear instead of reduced shear.

At first glance the 3D large scale structures in the Universe seem to make the lens equation, which uses the thin lens model, unusable. However, as light travels through a part of the Universe, we can assume, that part is separate from the others and apply the thin lens model to it. This is analogous to the Born approximation in quantum mechanics. This assumption is based on the following facts:

The Universe on large scales is homogeneous and the largest structures are significantly smaller than the horizon size. The potential inhomogeneities are weak and change slowly with spatial position.

Over the course of light's journey there can be many infinitesimally thin lenses and the sum of their convergence contributions make up that of the entire intervening large scale structure. As a result, the effective convergence is written in terms of the comoving angular diameter distance, $f_{\rm K}(\chi)$, the matter density contrast δ, the scale factor, a, the matter density parameter, $\Omega_{\rm m}$, the Hubble constant, H_0, and a weight function, $g(\chi)$, which is the source–redshift distribution weighted with the lens efficiency factor,

$$\kappa(\boldsymbol{\theta}) = \int_0^{\chi_{\rm h}} {\rm d}\chi \, p_\chi(\chi) \, \kappa(\boldsymbol{\theta}, \chi) \tag{48}$$

$$\kappa(\boldsymbol{\theta}) = \frac{3H_0^2\Omega_{\rm m}}{2c^2} \int_0^{\chi_{\rm h}} {\rm d}\chi \, g(\chi) \, f_{\rm K}(\chi) \frac{\delta(f_{\rm K}(\chi)\,\boldsymbol{\theta}, \chi)}{a(\chi)} \quad , \tag{49}$$

with

$$g(\chi) = \int_\chi^{\chi_{\rm h}} {\rm d}\chi' \, p_\chi(\chi') \, \frac{f_{\rm K}(\chi'-\chi)}{f_{\rm K}(\chi')} \quad , \tag{50}$$

where $\chi_{\rm h}$ is the comoving horizon scale, and $p_\chi(\chi){\rm d}\chi = p_{\rm z}(z){\rm d}z$ is the source redshift distribution.

8. Two-Point Statistics

As in most fields of cosmology, cosmic shear studies make use of statistical methods, since the original shape of a galaxy is not known, and consequently no single ellipticity measurement can provide any cosmic shear information to the observer. Nevertheless, for an isotropic Universe, the ensemble average of the main cosmic shear observable (the ellipticity of the galaxies) averages to zero.

Here we focus on real space tools, which are the standard statistical measurements that one commonly uses for weak lensing analysis. These are generally insensitive to masks, which are always present in the observations.

The two-point statistical properties of galaxy ellipticities are completely quantified by the two-point correlation functions (2PCFs),

$$\xi_{\pm}(\theta) = \langle \gamma_{\rm t}\gamma_{\rm t}\rangle(\theta) \pm \langle \gamma_{\times}\gamma_{\times}\rangle(\theta), \tag{51}$$

$$\xi_{\times}(\theta) = \langle \gamma_{\rm t}\gamma_{\times}\rangle(\theta) \ , \tag{52}$$

which correlate the tangential and cross components of the shear, $\gamma_{\rm t/x}$ (Eq. 47), of two galaxies separated by an angle θ in the sky. The tangential and cross components of the shear are measured with respect to the line connecting the two galaxies. Furthermore, since cosmologists believe that the Universe is parity invariant, the $\xi_{\times}$ vanishes, and we are left with $\xi_{\pm}$.

To make the connection between the 2PCFs and the underlying matter distribution let us first consider the relation between shear and convergence. To find this relation it is more practical to use the following notation which is equivalent to what we had earlier. From Eq. (16) we can see the following relation between shear, convergence and the lensing potential,

$$\gamma = \frac{1}{2}\partial\partial\psi \ , \ \kappa = \frac{1}{2}\partial^2\psi \ , \tag{53}$$

with

$$\partial = \partial_1 + i\partial_2 \ , \ \partial^* = \partial_1 - i\partial_2 \text{ and } \partial^2 = \partial\partial^* = \nabla^2 \ , \tag{54}$$

where $\partial_{1,2}$ is the partial derivative with respect to θ_1, θ_2. Eliminating ψ in Eq. (53) results in a relation between the shear and convergence,

$$\kappa = \partial^* \partial^* \partial^{-2} \gamma, \tag{55}$$

where the inverse Laplacian operator is

$$\partial^{-2} \equiv \int \frac{\mathrm{d}^2 \boldsymbol{\vartheta'}}{2\pi} \ln \left| \boldsymbol{\vartheta} - \boldsymbol{\vartheta'} \right| . \tag{56}$$

In Fourier space the relation between κ and γ is more straightforward. Using the relation between the partial derivatives in real space with their Fourier counterparts

$$\mathcal{F}(\partial) = i\hat{\ell} \, , \; \mathcal{F}(\partial^*) = i\hat{\ell}^* \, , \tag{57}$$

where

$$\hat{\ell} = \ell_x + i\ell_y \, , \; \hat{\ell}^* = \ell_x - i\ell_y \, , \tag{58}$$

we find

$$\hat{\gamma}(\boldsymbol{\ell}) = \mathrm{e}^{2\mathrm{i}\phi_\ell} \hat{\kappa}(\boldsymbol{\ell}) \, , \tag{59}$$

where ϕ_ℓ is the polar angle of $\boldsymbol{\ell}$, $\hat{\kappa}$ and $\hat{\gamma}$ are the Fourier transforms of κ and γ. Consequently assuming a flat sky,

$$\left\langle \hat{\kappa}(\boldsymbol{\ell}) \, \hat{\kappa}^*(\boldsymbol{\ell'}) \right\rangle = \left\langle \hat{\gamma}(\boldsymbol{\ell}) \, \hat{\gamma}^*(\boldsymbol{\ell'}) \right\rangle = (2\pi)^2 \delta_{\mathrm{D}}(\boldsymbol{\ell} - \boldsymbol{\ell'}) \, P_\kappa(\ell) \, , \tag{60}$$

where $P_\kappa(\ell)$ is the convergence power spectrum and is related to the matter power spectrum, $P_\delta(k)$, via the Limber equation with a certain choice of weight functions,

$$P_\kappa(\ell) = \frac{9H_0^4\Omega_{\rm m}^2}{4c^4}\int_0^{\chi_{\rm h}} {\rm d}\chi\ \frac{g^2(\chi)}{a^2}\ P_\delta\left(\frac{\ell}{f_{\rm K}(\chi)}, \chi\right)\ . \tag{61}$$

The above equation can be derived from Fourier transforming Eq. (48), for the convergence. Therefore, the 2PCFs are related to P_δ, but also to P_κ, given by

$$\xi_+(\theta) = \int_0^\infty \frac{{\rm d}\ell\,\ell}{2\pi}\ {\rm J}_0(\ell\theta)\ P_\kappa(\ell) \tag{62}$$

$$\xi_-(\theta) = \int_0^\infty \frac{{\rm d}\ell\,\ell}{2\pi}\ {\rm J}_4(\ell\theta)\ P_\kappa(\ell)\ , \tag{63}$$

where ${\rm J}_n$ is the n-th order Bessel function of the first kind.

In practice the 2PCFs are measured by correlating ellipticities of galaxies,

$$\xi_\pm(\theta) = \langle\epsilon_{\rm t}\epsilon_{\rm t}\rangle(\theta) \pm \langle\epsilon_\times\epsilon_\times\rangle(\theta), \tag{64}$$

which on average can be written in terms of their intrinsic ellipticity and shear, which in the case of mean shear reduces from Eq. (**??**) to

$$\epsilon = \epsilon_{\rm int} + \gamma\ . \tag{65}$$

By doing so a term containing the shear-shear correlation is produced along with other terms containing $\epsilon_{\rm int}$. The ellipticity correlation then can be written as,

$$\langle\epsilon\epsilon\rangle = \langle\gamma\gamma\rangle + \langle\epsilon_{\rm int}\epsilon_{\rm int}\rangle + \langle\epsilon_{\rm int}\gamma\rangle + \langle\gamma\epsilon_{\rm int}\rangle\ . \tag{66}$$

The first term is the quantity that we need, while the other terms contaminate the estimated 2PCFs. The second term in the above equation is the intrinsic-intrinsic correlation (II), which is only important for pairs of galaxies which are physically close in space and their intrinsic shape and orientation is affected by the same gravitational potential. Depending on which of the galaxies is closer to the observer one of the third or fourth terms vanish. Since the intrinsic shape of a background galaxy has no correlation with the shear of a foreground galaxy, only one of these terms is important. A background galaxy shape is sheared by the same gravitational field that a foreground galaxy resides in. This correlation (GI) can have an amplitude comparable to the first term.

9. Observing weak lensing

Consider an isolated galaxy with surface brightness $I(\boldsymbol{\theta})$. We can define its shape through the quadrupole moment of the light distribution,

$$Q_{ij} = \frac{\int d^2\theta\, I(\boldsymbol{\theta})\theta_i\,\theta_j}{\int d^2\theta\, I(\boldsymbol{\theta})} \tag{67}$$

and an ellipticity from its axis ratio η (major axis / minor axis) and orientation ϕ,

$$\left(\begin{array}{c} e_1 \\ e_2 \end{array}\right) = \frac{1-\eta}{1+\eta}\left(\begin{array}{c} \cos 2\phi \\ \sin 2\phi \end{array}\right) = \frac{1}{N}\left(\begin{array}{c} Q_{11}-Q_{22} \\ 2Q_{12} \end{array}\right) \tag{68}$$

For a perfect ellipse we have written the ellipticity in terms of Q_{ij} where $N = Q_{11}+Q_{22}+2(Q_{11}Q_{22}-Q_{12}^2)^{1/2}$. Figure 9 shows these ellipticity parameters for a series of ellipses.

How is the ellipticity of the galaxy that we observe related to its intrinsic ellipticity before it was lensed? For this we use the Jacobian to transform the image quadrupole moments ,

$$Q^s_{ij} = A_{il}Q_{lm}A_{mj}\,. \tag{69}$$

and calculate the intrinsic ellipticity of the source e^s in terms of the observed ellipticity e and the reduced shear g. In the weak gravitational lensing limit ($\kappa << 1$) Schneider & Seitz (1995) show that,

$$e^s = e - g\,. \tag{70}$$

This wonderfully simple relationship means that if all sources were circular ($e^s = 0$) a measure of the lensed galaxy ellipticity directly recovers the gravitational shear g and hence the underlying gravitational potential. In practice galaxies have a intrinsic shape, but averaged over many galaxies $< e^s >= 0$. We can therefore determine g by measuring the average ellipticity of a large sample of galaxies.

10. Dark matter mapping

Up to this point we have focused on extended but discrete lens systems: the strong lensing cluster, the weak lensing galaxy halo. Weak lensing also has the ability map out the extended large scale structure of the Universe. Lensing is unique in this respect as it is sensitive to all matter irrespective of its state or nature. Whilst the derivation of the lens theory for large scale structure differs somewhat from our derivations thus far (we can no longer assume that the deflection of light rays is small compared to the scale on which the lens mass distribution changes), the fundamental results remain unchanged and we will use them. For a full derivation see Bartelmann & Schneider (2001).

Statistically we can observe a weak shear distortion γ from the shapes of distant galaxies. What we want to measure is the distribution of mass or the convergence κ, as shown in Figure 10. Kaiser & Squires (1993) were the first to show that you can "invert" a map of a varying shear field across to sky to produce a map of the varying mass distribution as follows:

We can derive a relationship between convergence and shear using the lensing potential (go back to Bartelmann & Schneider 2001 or my thesis if you want the details). Writing the deflection angle in terms of κ we have

$$\alpha(\boldsymbol{\theta}) = \nabla\psi(\boldsymbol{\theta}) = \frac{1}{\pi}\int d^2\theta'\,\kappa(\boldsymbol{\theta'})\frac{\boldsymbol{\theta}-\boldsymbol{\theta'}}{|\boldsymbol{\theta}-\boldsymbol{\theta'}|^2}\,, \tag{71}$$

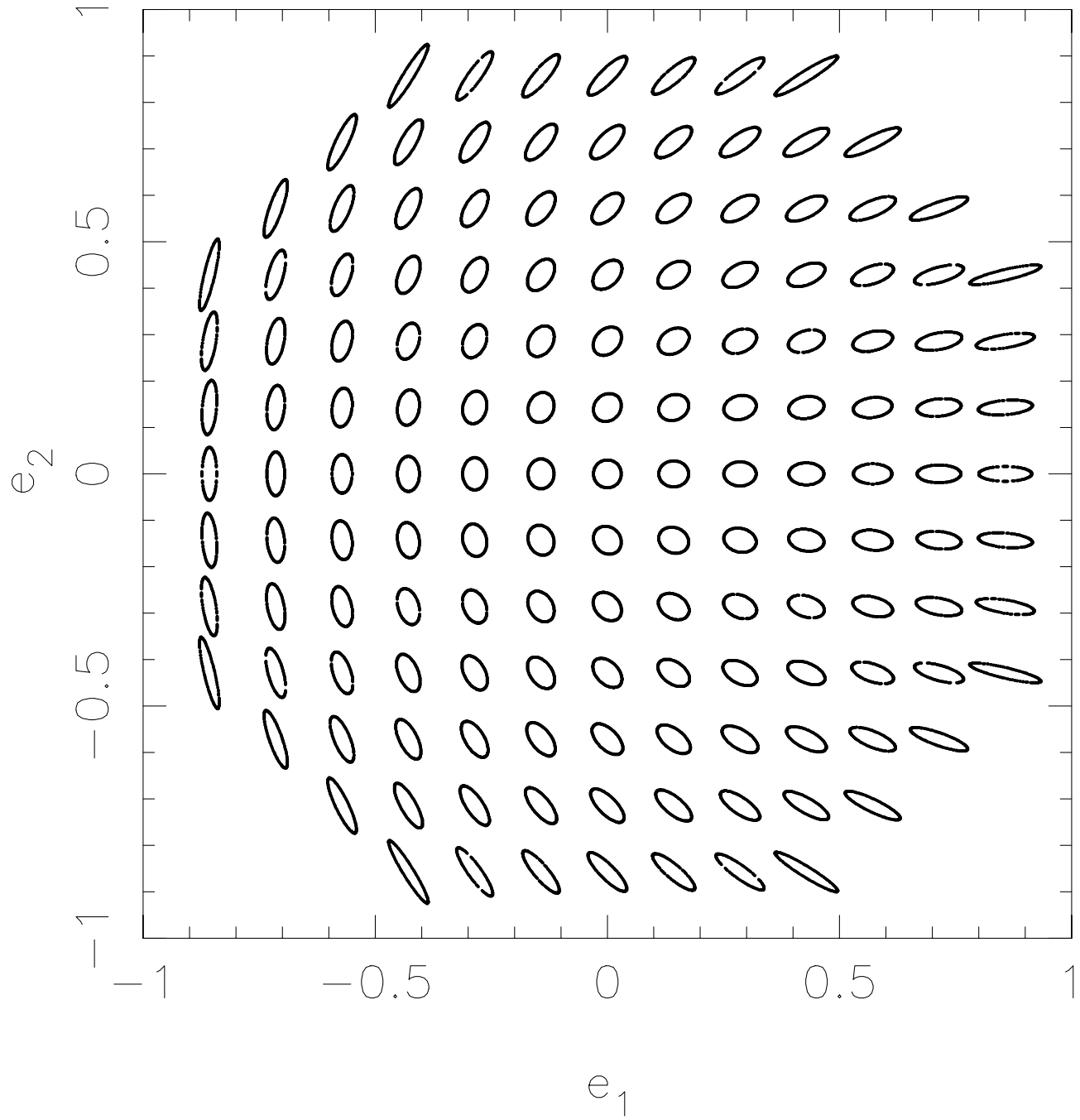

Figure 9. Ellipticity parameters for a series of ellipses

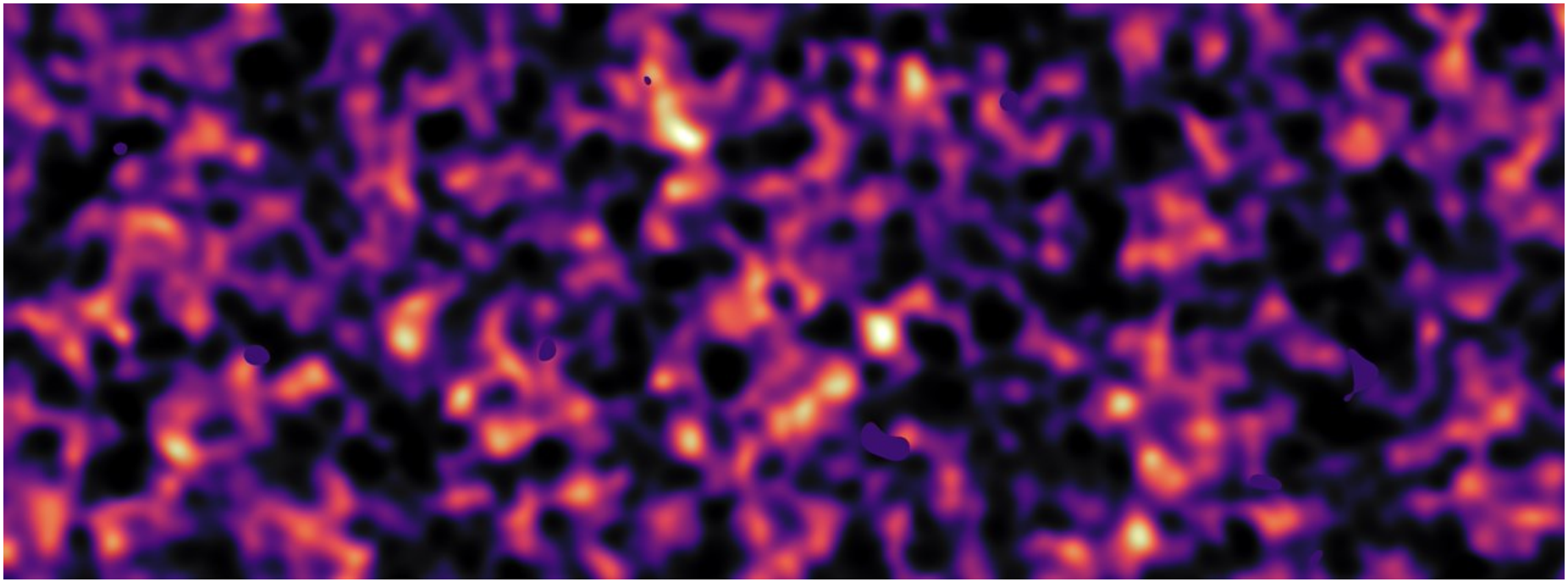

Figure 10. The dark matter κ mapped by the Kilo-Degree survey (Hildebrandt et al 2017). This image reconstruction was made by analysing the light collected from over three million distant galaxies more than six billion light years away.

and the second derivatives of the lensing potential are then

$$\psi_{i,j} = \frac{1}{\pi}\int d^2\theta'\,\kappa(\boldsymbol{\theta'})\left[\delta_{ij}\frac{1}{|\boldsymbol{\theta}-\boldsymbol{\theta'}|^2} - 2(\theta_i-\theta'_i)(\theta_j-\theta'_j)\frac{1}{|\boldsymbol{\theta}-\boldsymbol{\theta'}|^4}\right]. \tag{72}$$

Writing the two shear components in terms of the 'complex' shear $\gamma = \gamma_1 + i\gamma_2$ and recalling that $2\gamma_1 = (\psi_{,11} - \psi_{,22})$ and $\gamma_2 = \psi_{,12}$ we can directly relate what we observe (γ) to what we want to know (κ).

$$\gamma(\boldsymbol{\theta}) = \frac{1}{\pi}\int d^2\theta'\,D(\boldsymbol{\theta}-\boldsymbol{\theta'})\kappa(\boldsymbol{\theta'})\,, \tag{73}$$

where the window function $D(\boldsymbol{\theta}) = -(\theta_1 - i\theta_2)^{-1}$. This is solved in Fourier space

$$\hat{\kappa}(k) = \frac{1}{\pi}\hat{D}^*(k)\hat{\gamma}(k)\,, \tag{74}$$

where $\hat{D}(k)$ is the Fourier transform of the window function. To make a mass map we therefore need to

- Obtain high resolution imaging of a large area of sky.
- Detect and measure the ellipticity e of all the resolved galaxies.
- Grid up the field and average e within cells to get $\gamma(\boldsymbol{\theta})$.
- Take the Fourier transform of $\gamma(\boldsymbol{\theta})$ and multiply by the window function to get $\hat{\kappa}(k)$.

- Fourier transform back an you have a map of the varying density $\kappa(\boldsymbol{\theta})$ across your patch of sky.

Unfortunately in practice this is not as easy as it sounds due to finite fields and masked holes in the data. The majority of research in this area therefore builds on this theory to make it more applicable to real data. This theory can also be extended to three dimensions (note κ is the projected surface mass density so the reconstructions described above are in 2D). Full 3-D reconstructions of the dark matter density requires the best data and to date has only been attempted using deep surveys from the Hubble Space Telescope.

11. A bluffers guide to the matter power spectrum

The matter power spectrum $P_\delta(k, z)$ contains all the key information we want to know about the Universe and is at the basis of many cosmological analyses. It is however just a statistical tool with which to characterise the density fluctuations in the universe. You can imagine it just as a count, telling us how many large scale fluctuations there are (i.e galaxy clusters), and small scale fluctuations (i.e galaxies). It has a characteristic shape which can be quite easily understood by considering how matter density fluctuations grow and evolve (i.e get more dense) with time.

A fluctuation at position $\mathbf{x}$ produces a matter density contrast such that

$$\delta(\mathbf{x}) = \frac{\rho(\mathbf{x}) - \bar{\rho}}{\bar{\rho}}. \tag{75}$$

Provided that $\delta \ll 1$, perturbation theory, shows that adiabatic matter density fluctuations will grow according to

$$\begin{array}{lllll} \delta(a) & \propto & a^2, & a < a_{\rm eq} & \text{before equality} \\ \delta(a) & \propto & a, & a > a_{\rm eq} & \text{after equality,} \end{array} \tag{76}$$

Figure 11 shows a sketch of perturbation growth. Until matter domination the expansion time-scale, determined by the radiation density, is shorter than the collapse time-scale of the dark matter. Hence the fast radiation driven expansion will prevent the growth of dark matter perturbations. This however will only affect the perturbations which are smaller than the regions over which light or radiation can travel. These causally connected regions are determined by the horizon size d_H, and larger scale perturbations with wavelength $\lambda > d_H$ will remain unaffected, growing in amplitude as given by equation 76. As the horizon scale grows with time, more perturbations enter the horizon and their growth is stalled until matter equality. This results in the overall suppression of the amplitude of fluctuations which enter the horizon before matter radiation equality by a factor

$$f_{\rm sup} = \frac{a_{\rm enter}}{a_{\rm eq}} \propto k^{-2} \tag{77}$$

This will affect the largest k-scales first (the smallest physical scales), and so we'll see a turnover in the power spectrum

$$P_\delta(k >> k_0) = f_{\rm sup}^2 P_i(k) \propto k^{-3} \tag{78}$$

where the Harrison-Zeldovich initial power spectrum $P_i(k) \propto k^{-1}$, is derived from the theory that at the start of the Universe the amplitude or power of a given scale fluctuation is always the same when it enters the horizon.

The modification to the initial power spectrum during radiation domination, that has just been described, is formally contained in the transfer function T such that

$$P_\delta(k, z) = T(k, z)^2 P_i(k), \tag{79}$$

where T is dependent on the constituents of the Universe.

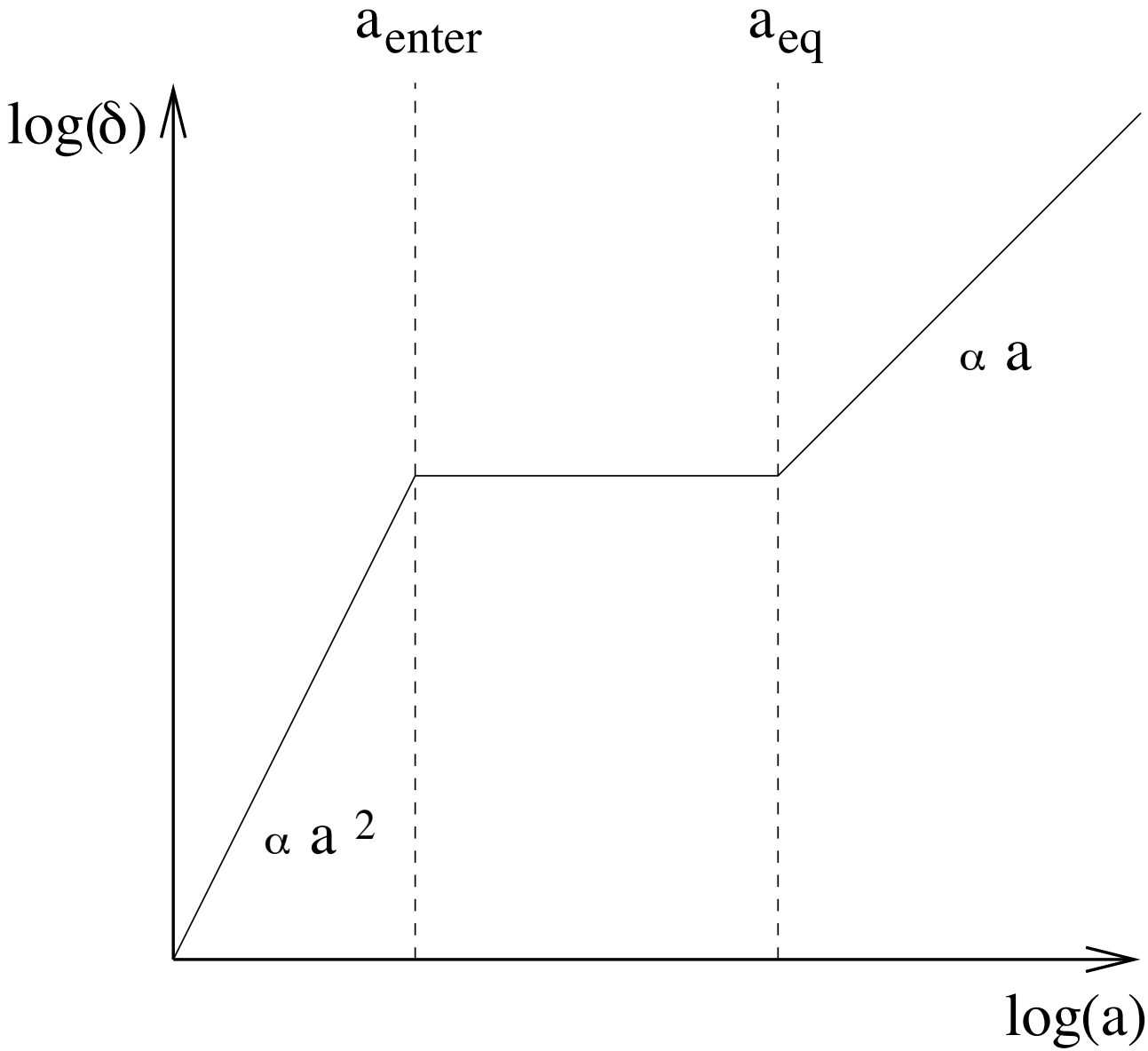

Figure 11. Schematic of the suppression of fluctuation growth during the radiation dominated phase when the density perturbation enters the horizon at $a_{\rm enter} < a_{\rm eq}$. The rapid radiation driven expansion prevents the perturbation from growing until matter radiation equality.

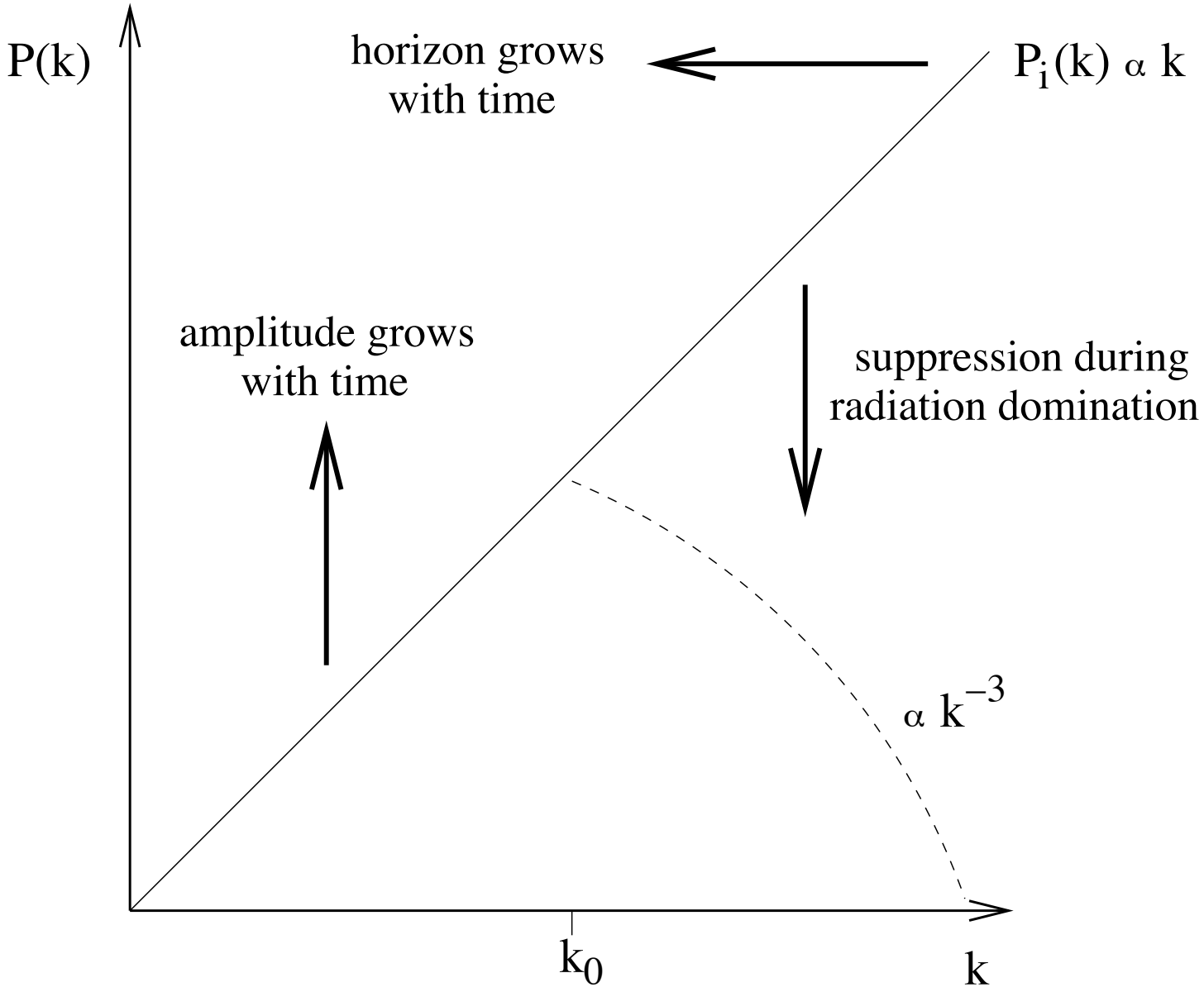

Figure 12. Schematic of the modification to the initial scale invariant power spectrum, (note log scale).

12. Weak lensing by Large Scale Structure: Cosmological parameters

Weak lensing gives us an unbiased measurement of the matter distribution and hence the underlying matter power spectrum. We can therefore use it to constrain cosmological parameters and it is particularly sensitive to a combination of the matter density Ω_m and the normalisation of the matter power spectrum σ_8. This is because lensing is sensitive to both mass (Ω_m) and its distribution (σ_8). Stronger clustering results in a higher fraction of regions with strong shear. To constrain cosmological parameters we typically use 2pt statistics. We'll focus on the 2pt shear correlation function ξ which can be estimated from the data using

$$\xi_+(\theta) = \sum_{\alpha=1}^{2} \frac{\sum_{\rm pairs} \mathrm{e}_\alpha(\boldsymbol{x})\, \mathrm{e}_\alpha(\boldsymbol{x}+\boldsymbol{\theta})}{N_{\rm pairs}}\,. \tag{80}$$

Figure **??** shows the most recent measurement of this statistic from the Kilo-Degree Survey (KiDS). On small angular scales we see galaxy shapes are very correlated (their light has been distorted by the same intervening matter). On large angular scales the correlation weakens as the galaxies are lensed by different structures that are only weakly correlated.

It can be shown (Bartelmann & Schneider 2011 and in detail in my thesis amongst other places) that the 2pt shear correlation function is related to the matter power spectrum

$$\xi_+(\theta) = \frac{1}{2\pi} \int dk\, k\, P_\kappa(k)\, J_0(k\theta), \tag{81}$$

where J_0 is the zeroth order Bessel function and P_κ is the power spectrum of the convergence,

$$P_\kappa(l) = \frac{9H_0^4\Omega_m^2}{4c^4} \int_0^{w_H} dw\, \frac{g^2(w)}{a^2(w)}\, P_\delta\left(\frac{l}{f_K(w)}, w\right)\,, \tag{82}$$

P_δ is the 3D matter power spectrum, $f_K(w)$ is the comoving angular diameter distance out to a radial distance w, and $g(w)$ is a weighting function that depends on the redshift distribution of the survey (Bartelmann & Schneider 2001).

A measurement of the correlation between galaxy ellipticities can therefore be directly related to the underlying matter power spectrum! Figure 14 shows the cosmological constraints from this data set compared to constraints from the CMB.

12.1. Dark energy and modified gravity

We have shown that weak lensing can probe dark matter but what about dark energy? Dark energy acts to oppose the clustering of dark matter over time, suppressing the growth of structure. In addition dark energy changes the distance-redshift relation. Lensing is sensitive to both these effects and in the future will be able to set very tight constraints on the properties of dark energy. The other main probes of dark energy are supernovae or baryon acoustic oscillations. These probes are only sensitive to the distance-redshift relation and cannot distinguish between the cosmological constant or a modification to our theories of gravity. If we find that the constraints from lensing (based on GR) are in disagreement with those from distance-redshift probes this would be evidence for a new beyond-Einstein model of gravity.

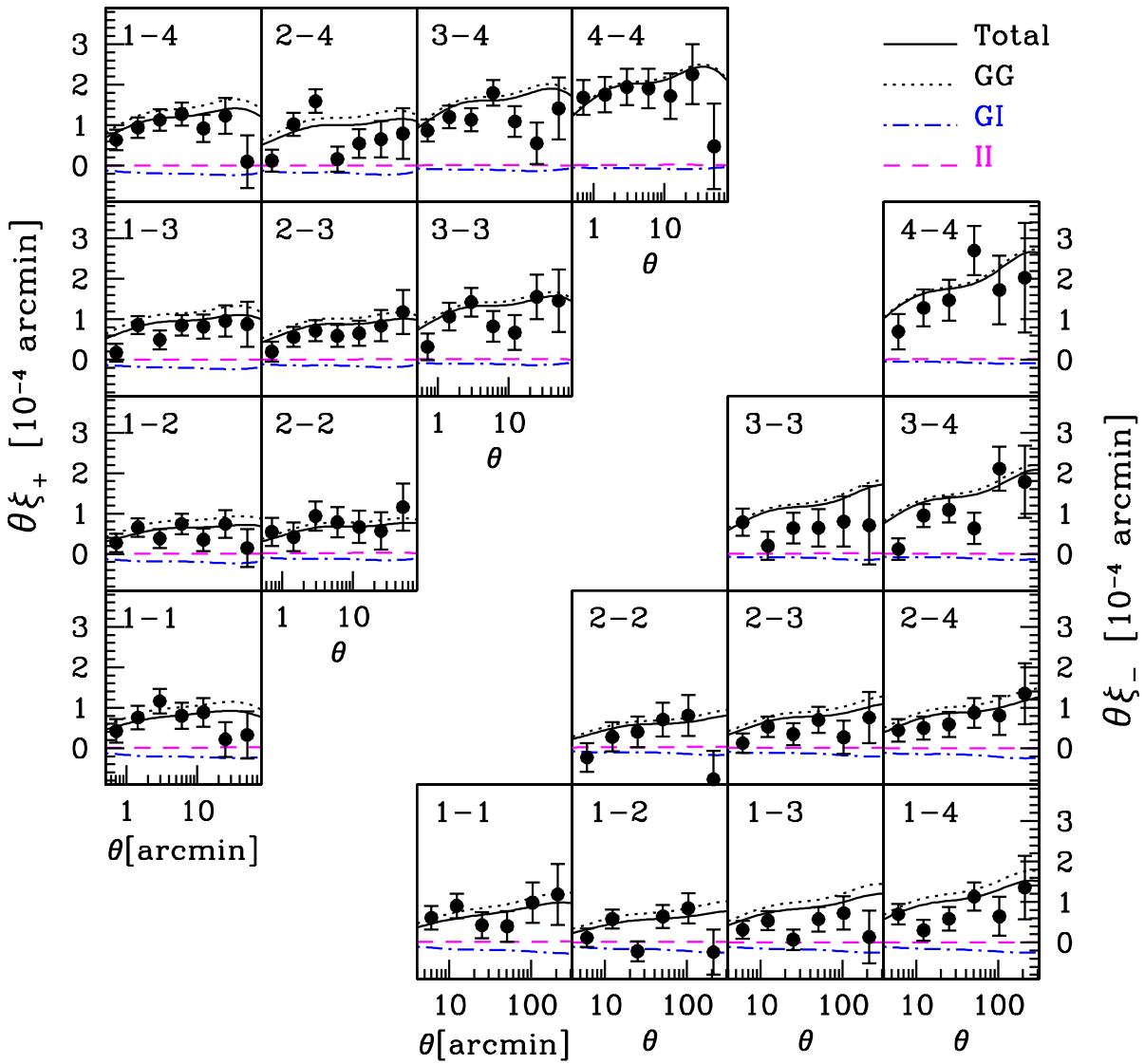

Figure 13. Tomographic measurements of ξ_+ (upper-left panels) and ξ_- (lower-right panels) from the full KiDS-450 dataset. The theoretical model (solid) has $\Omega_m = 0.25$ and $\sigma_8 = 0.85$ and is composed of a cosmic shear term (GG, dotted), and two intrinsic alignment terms (GI, dot-dashed, and II, dashed). Figure taken from Hildebrandt et al (2017).

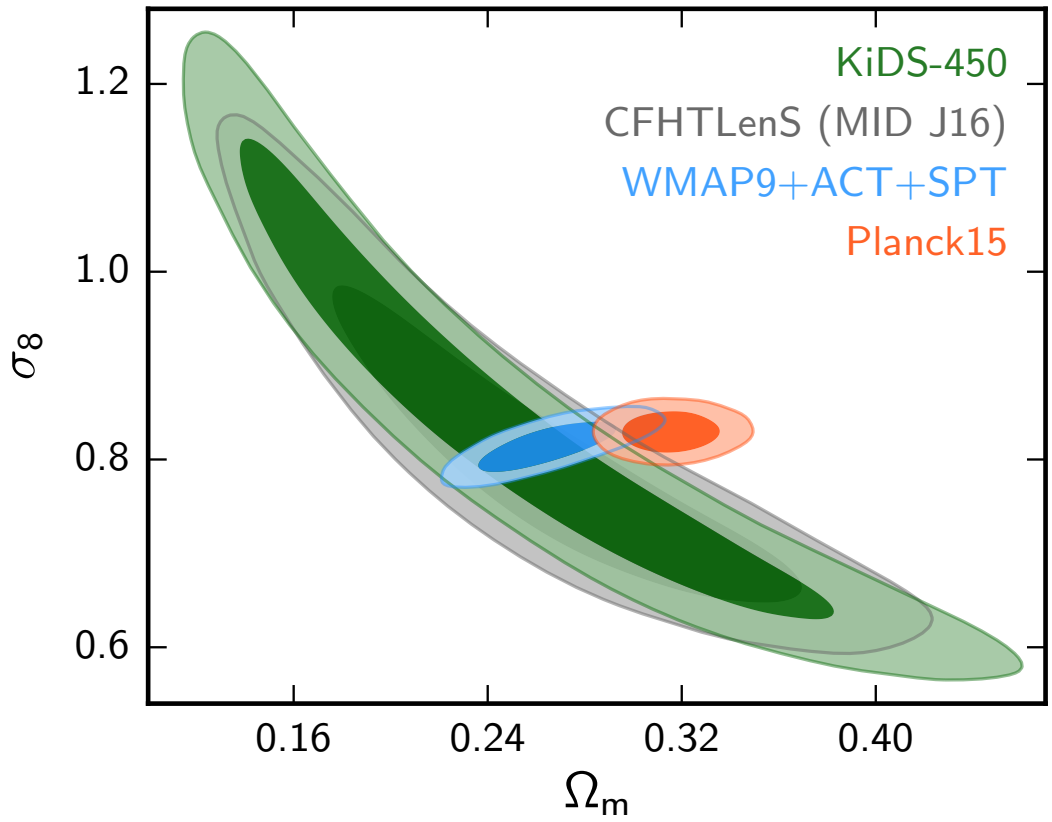

Figure 14. Constraints on the matter density parameter Ω_m and the normalisation of the matter power spectrum σ_8 from weak lensing (KiDS survey, green, CFHTLenS in grey), and the CMB (WMAP9, blue, Planck, red). Figure taken from Hildebrandt et al (2017).

12.2. Systematics

Gravitational lensing has been heralded as the most powerful technique for studying the dark universe, but it is also the most technologically challenging. The typical distortion induced by dark matter, as a galaxyÕs light travels through the Universe, changes the ellipticity of that galaxy by less than 1%. In the last few moments before that light is captured on Earth, the atmosphere, telescope and detector can together change the ellipticity of the galaxy by 10% or more. In order to isolate the alignment signature that dark matter imprints, we need to model all the distortions introduced by technology and the atmosphere to very high precision and then invert these terrestrial effects to accurately recover the cosmological signal. Just to up the ante, the terrestrial effects change every second as the wind and ground temperature alters the density of the air in different layers of the atmosphere, and the telescope slowly moves to track the rotation of the Earth.

Furthermore, this lensing effect is so weak, that to detect it we need to analyse the images of hundreds of millions of galaxies, which involves rapidly processing peta-bytes of data. For the past decade, astronomers have been setting Òbig dataÓ challenges, see Figure 15, to crowd-source the best minds to solve this monumental computational task. The Kaggle ÒMapping Dark MatterÓ Challenge saw 700 non-astronomers competing for a prized tour around NASAÕs Jet Propulsion Lab. Their submissions fuelled a new range of machine-learning ideas for the astronomers to put into practice.

One final astrophysical challenge persists, which the astute reader will have already recognised. What if our assumption that galaxies are randomly oriented throughout the universe is wrong? We know that the way galaxies form and evolve depends on their local environment, and hence two galaxies in the same district of the universe may well have a natural born alignment with each other. We have measured this effect by looking at the alignment of galaxies in tight-knit communities, in contrast to the alignment of galaxies widely dispersed through the Universe. What we found was that the average natural alignment between galaxies is roughly 100 times smaller than the observed alignment that dark matter induces (see Heymans et al 2013). This is small, but not small enough to ignore. Current research focuses on ensuring these sources of systematics can be minimised and accounted for in preparation for the next generation of lensing telescopes that are being built to “observe” the Dark Universe.

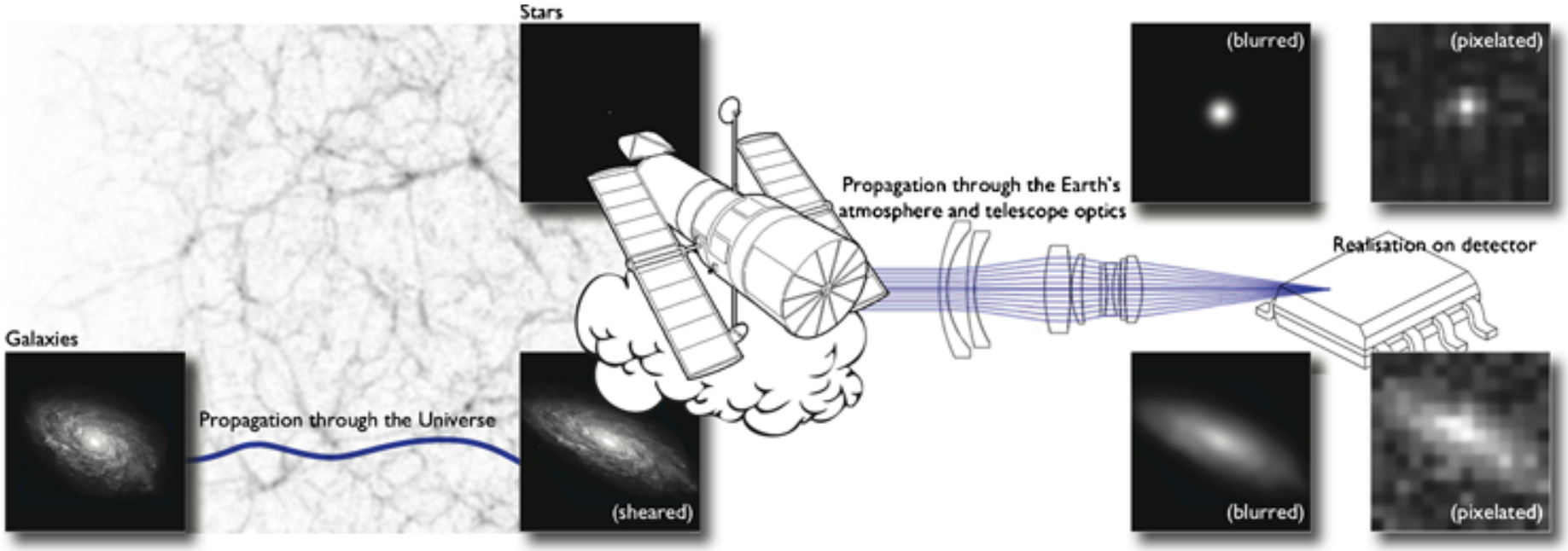

Figure 15. Summary of the main effects on an individual galaxy or star. The GREAT challenges seek to estimate the shear distortion applied to a galaxy image, correcting for the additional effects in the EarthÕs atmosphere and telescope optics, which are also experienced by the images of stars; for space-based telescopes the atmospheric effects are not present so that telescope and detector effects alone induce a PSF. Image from Kitching et al 2010

13. The future

Three lensing teams are currently competing to be the first to reveal the next major leap in our understanding of the dark universe. The Europeans, with the Kilo-Degree Survey, and the Japanese, with the Hyper-Suprime Camera survey, are imaging 1500 square degrees of the cosmos Đ nearly 5% of our sky and

10 times as much sky as our current best lensing survey. The US, with the Dark Energy Survey, will eventually cover 3 times that area. All three surveys will conclude their observations over the next few years. There is great interest in whether these surveys will uncover the same ÒtensionÓ that we see between current lensing observations of the invisible dark universe and the Planck satelliteÕs observations of the cosmic microwave background. Gravitational-lensing surveys are very sensitive to how dark matter clumps, but Planck prefers a much clumpier Universe than the lensing surveys are currently seeing. This lack of agreement could mean a flaw in one or both of the methods. If it persists, as the methods and data quality improve, it has been speculated that this could be evidence for the existence of a new type of neutrino called the sterile neutrino.

Over the next decade, three new major international projects will work in tandem in the final stages of our quest to understand the dark side. The Euclid satellite will be launched above the atmosphere, providing Hubble-Space-Telescope-quality imaging across the whole sky. Getting above the atmosphere gives us a much clearer view of the Universe, and the keen vision of Euclid will be extremely sensitive to the weak dark matter distortions that we are trying to detect. It will also measure the spectra Ð and hence redshift and distance information Ð of millions of galaxies with which to chart the expansion of the Universe. The Large Synoptic Survey Telescope will image the whole southern sky every three nights and provide deep multi-colour imaging with which to measure distances to the galaxies without spectra. Not only will this allow us to chart the evolution of dark matter structures, but this telescope will also be able to detect killer rocks in our solar system that may one day obliterate planet Earth! The Square Kilometre Array will provide high- resolution imaging in the radio part of the electromagnetic spectrum, with precision redshift and polarisation observations that will allow us to untangle the lensing alignment signature of dark matter from naturally arising alignments. In combination, these surveys will be able to use gravitational lensing to map dark matter and dark energy over the last 10 billion years in the history of the universe, testing gravity on the largest of scales in space and time.

14. Reviews

The "Bible" of Gravitational Lensing is still the Bartelmann & Schneider Review of 2001. Very little beats that on the theory side of things. For a more uptodate observations review, Wienberg et al 2013 is excellent. Kilbinger 2015 presents a thorough review of the field of cosmic shear measurements and Mandelbaum 2017 reviews all the the different systematics and mitigations strategies available to ensure that your that weak lensing measurements are truely cosmic!

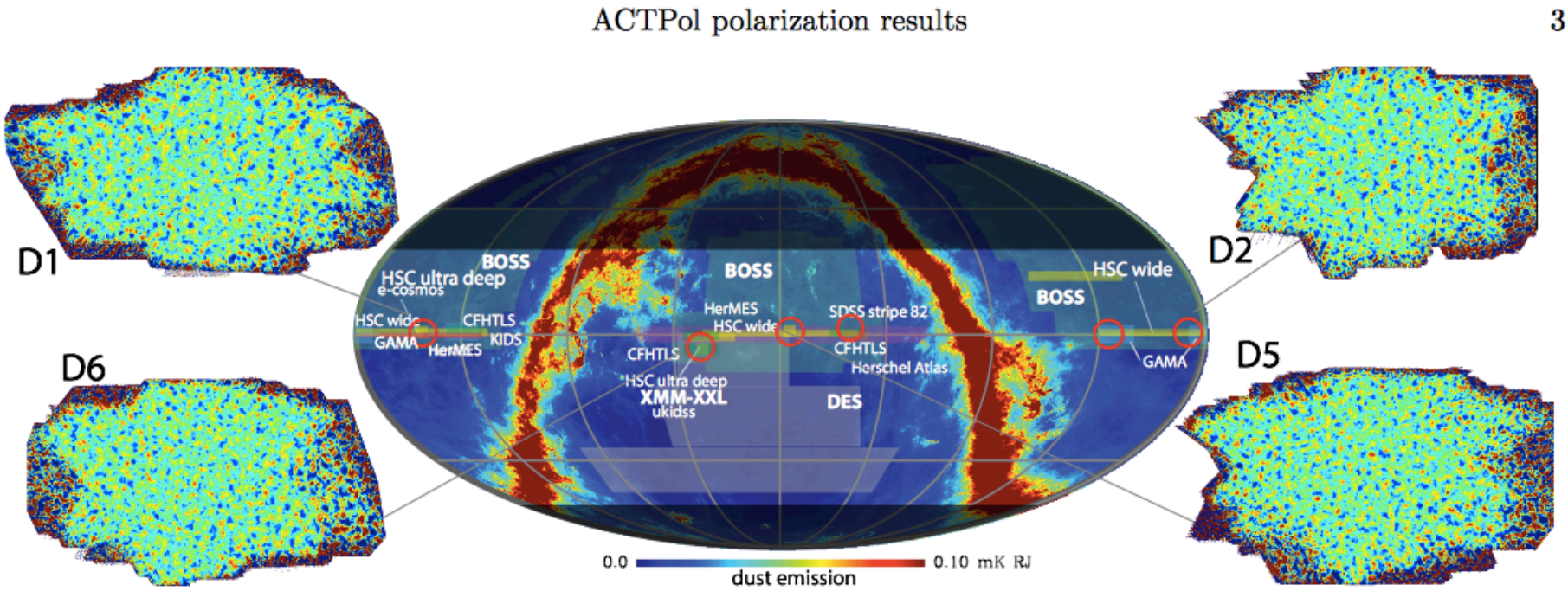

Figure 16. Figure from Naess et al 2014